Hippocampal interneurons are direct targets for circulating glucocorticoids

Kimberly L. Kraus[1,2,3],

Arihant P. Chordia[1],

Austin W. Drake[1,2,3],

James P. Herman[4],

Steve C. Danzer[1,2,3,5,*]

[1]Cincinnati Children's Hospital, Department of Anesthesia, Cincinnati, Ohio

[2]University of Cincinnati College of Medicine, Medical Scientist Training Program, Cincinnati, Ohio

[3]University of Cincinnati College of Medicine, Neuroscience Graduate Program, Cincinnati, Ohio

[4]University of Cincinnati College of Medicine, Department of Pharmacology and Systems Physiology, Cincinnati, Ohio

[5]University of Cincinnati College of Medicine, Department of Anesthesiology, Cincinnati, Ohio

Abstract

The hippocampus has become a significant target of stress research in recent years because of its role in cognitive functioning, neuropathology, and regulation of the hypothalamic pituitary adrenal (HPA) axis. Despite the pervasive impact of stress on psychiatric and neurological disease, much of the circuit- and cell-dependent mechanisms giving rise to the limbic regulation of the stress response remain unknown. Hippocampal excitatory neurons generally express high levels of glucocorticoid receptors (GRs) and are therefore positioned to respond directly to serum glucocorticoids. These neurons are, in turn, regulated by neighboring interneurons, subtypes of which have been shown to respond to stress exposure. However, GR expression among hippocampal interneurons is not well characterized. To determine whether key interneuron populations are direct targets for glucocorticoid action, we utilized two transgenic mouse lines to label parvalbumin (PV+) and somatostatin (SST+)-positive interneurons. GR immunostaining of labeled interneurons was characterized within the dorsal and ventral dentate hilus, dentate cell body layer, and CA1 and CA3 *stratum oriens* and *stratum pyramidale*. While nearly all hippocampal SST+ interneurons expressed GR across all regions, GR labeling of PV+

*Corresponding author Steve C. Danzer, PhD, 3333 Burnet Avenue, ML 2001 Cincinnati, Ohio 45229-3039 (513) 636-4526 (phone), (513) 636-7337 (fax), steve.danzer@cchmc.org.

interneurons showed considerable subregion variability. The percentage of PV+, GR+ cells was highest in CA3 *stratum pyramidale,* and lowest in CA1 *stratum oriens,* with other regions showing intermediate levels of expression. Together, these findings indicate that, under baseline conditions, hippocampal SST+ interneurons are a ubiquitous glucocorticoid target, while only distinct populations of PV+ interneurons are direct targets. This anatomical diversity suggests functional differences in the regulation of stress-dependent hippocampal responses.

Graphical Abstract.

Percentage of hippocampal parvalbumin (PV)-positive and somatostatin (SST)-positive interneurons which are positive for GR protein across dorsal and ventral hippocampal subregions (CA1, CA3, DG) and cell layers.
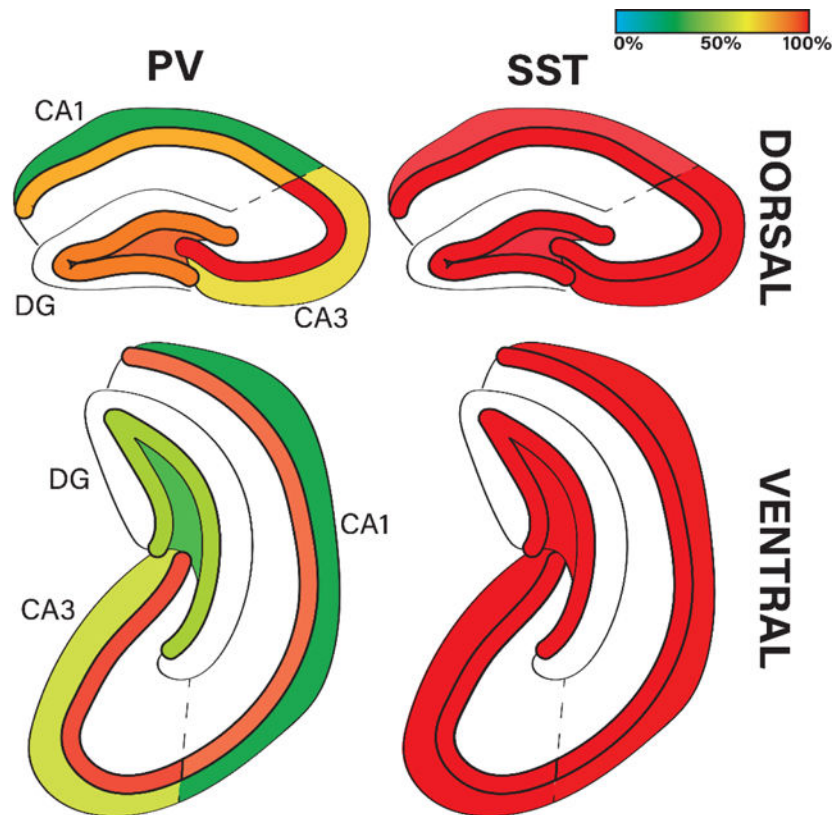
Keywords

glucocorticoid receptor (GR); stress; hippocampus; interneurons; parvalbumin (PV); somatostatin (SST)

INTRODUCTION

The intersection between stress and neurological disease has become a focal point of research in recent years as the influence of stress on health and wellness has become clear. Although proper hypothalamic-pituitary-adrenal (HPA) axis function regulates both normal

development and the body's response to challenges, dysregulation of the HPA axis has been linked to the pathophysiology of many neuropsychiatric disorders, such as depressive (Carroll et al., 1976), anxiety (Dieleman et al., 2015), and panic disorders (Erhardt et al., 2006). In addition to links between HPA axis dysregulation and disease incidence, exposure to both acute and chronic stressors can modulate disease severity, as has been explored in the context of epilepsy (Castro et al., 2012; Joëls, 2009). To improve our understanding and treatment of stress-dependent disease, it is necessary to reveal the cell- and circuit-level dynamics at play in the limbic regulation of the stress response.

The hippocampus is a key node within the limbic stress circuitry regulating the HPA axis, working in parallel with the amygdala and medial prefrontal cortex to influence HPA axis activation (Radley & Sawchenko, 2011; Ulrich-Lai & Herman, 2009). Although the modulatory role of the hippocampus is context-specific, it effectively acts as a brake on HPA axis drive, as stimulation of the hippocampus decreases glucocorticoid secretion, while lesions of the ventral subiculum increase glucocorticoid secretion (Dunn & Orr, 1984; Herman et al., 1989, 2003; Herman & Mueller, 2006; Rubin et al., 1966). Excitatory hippocampal dentate granule cells, CA1 pyramidal cells and, to a lesser extent, CA3 pyramidal cells all express glucocorticoid receptors (GRs), allowing them to respond directly to changes in stress-induced glucocorticoid secretion (Van Eekelen et al., 1988; Vandevyver et al., 2014). The hippocampus is also critically involved in the pathophysiology of numerous neurological diseases, including temporal lobe epilepsy and Alzheimer's disease. Therefore, glucocorticoids can regulate hippocampal function in both healthy and diseased states through direct action on excitatory glutamatergic neurons (Olijslagers et al., 2008; Pasricha et al., 2011).

While the expression and function of GR among hippocampal excitatory neurons has been explored in detail, its role among hippocampal inhibitory interneurons is poorly understood. Inhibitory interneurons are present among all excitatory cell layers of the hippocampus and are crucial for proper hippocampal circuit function. Together, multiple subtypes of interneurons are responsible for exerting robust feed-forward and feed-back inhibition, controlling the flow of information through the hippocampus (Booker & Vida, 2018). Given their prominent role in hippocampal physiology, it is important to determine whether interneurons are direct targets for glucocorticoid signaling.

For the present study, we used transgenic mouse models to label parvalbumin-(PV+) and somatostatin-positive (SST+) interneurons with eGFP. Specificity of the transgenic labeling approach was confirmed by PV and SST immunohistochemistry, followed by quantification of the percentage which were GR immunopositive. GR co-expression was quantified within three major hippocampal subregions across the dorsal and ventral hippocampus. Our data indicate significant heterogeneity of GR expression within and between interneuron subtypes, suggesting the potential for context-specific and stress-dependent regulation of hippocampal circuit excitability.

MATERIALS AND METHODS

Animals.

Male and female mice were maintained on a C57BL/6 background and housed in a sterile barrier facility at 72±2°F with same-sex littermates on a 14hr/10hr dark/light cycle with access to standard autoclaved rodent chow and water *ad libitum.* Three cohorts of mice were used over the course of this study (Table 1), as follows: **1) PV;eGFP**: parvalbumin (PV)-targeted conditional reporter mice were bred in-house by crossing hemizygous flippase-expressing Pvalb-2A-FlpE-D mice (B6.Cg-Pvalbtm2.1(flpe)Hze/J, Stock #: 021191, Jackson Laboratory) and hemizygous fritted eGFP reporter mice (Gt(ROSA)26Sortm1.2(CAG-EGFP)Fsh, Stock #:32038-JAX, Jackson Laboratory) to generate PV FlpO$^{+/-}$, eGFP$^{+/-}$ offspring. **2) SST;eGFP**: somatostatin (SST)-targeted conditional reporter mice were bred by crossing hemizygous Sst-ires-Flp ($Sst^{tm3.1(flpo)Zjh}$/J, Stock # 028579, Jackson Laboratory) and hemizygous fritted eGFP reporter mice to generate SST FlpO$^{+/-}$;eGFP$^{+/-}$ offspring. **3) GR$^{fl/fl}$**: a mating pair of homozygous floxed Nr3c1 mice (B6.Cg-*Nr3c1$^{tm1.1Jda}$*/J, Stock #: 021021) were ordered and maintained in-house. Offspring were crossed with C57BL/6 wild-type mice (Charles River) to generate heterozygous (GR$^{fl/wt}$) mating pairs yielding experimental (GR$^{fl/fl}$) and control (GR$^{wt/wt}$) littermates. All study mice were handled daily for 10 minutes for one week before euthanasia for histology. All experimental procedures and protocols were designed to minimize stress and discomfort and conducted as approved by the Cincinnati Children's Hospital Institutional Animal Care and Use Committee in accordance with NIH guidelines for the care and use of animals.

Tissue Collection.

Following 1 week of habituation, mice were overdosed with sodium pentobarbital (250 mg/kg, i.p.) within 10 minutes of cage disturbance and transcardially perfused with 50–75 mL ice-cold 1x phosphate-buffered saline (PBS) + 0.1% heparin followed by 100 mL of 2.5% paraformaldehyde (PFA) + 4% sucrose dissolved in 1XPBS. Brains were post-fixed for 12–18 hrs in 2.5% PFA + 4% sucrose before being transferred to 10%, 20% and 30% sucrose each subsequent 24-hr period. After cryoprotection, brains were frozen in isopentane at −35 to −45°C and stored at −80°C. Coronal sections were cut at 40 μm thickness with a cryostat (22–24°C), mounted onto gelatin-coated slides and stored at −80°C. Before immunohistochemistry, sections were thawed in 1XPBS for 10 minutes.

Immunohistochemistry.

Slide-mounted coronal sections were immunolabeled with polyclonal IgG primary antibodies against parvalbumin (PV) (1:1000) or glucocorticoid receptor (GR) (1:800) and monoclonal antibodies against somatostatin (SST) (1:200) or enhanced green fluorescent protein (eGFP) (1:500) (Table 2). All antibodies were assessed for cross-reactivity. Tissue was permeabilized in 3% Triton-X + 0.75% glycine solution overnight at 4°C, blocked (1.5% Triton-X, 5% normal goat serum [NGS], 0.75% glycine) overnight at 4°C under agitation, then incubated with primary antibody diluted in block for 72 hrs at 4°C under agitation. Slides were washed in block and incubated with one of the following highly cross-adsorbed Alexa-Fluor secondary antibodies (1:1000, diluted in 1XPBS): goat anti-rabbit

647, goat-anti guinea pig 647, goat anti-chicken 488 and goat anti-rat 568 (Table 2). Slices were washed and mounted with ProLong Glass Antifade mountant with Nuclear Blue stain (Thermo Fisher Scientific, Cat# P36981), cover slipped with Fisherbrand 1.5 mm cover glass, sealed with clear nail polish, and stored flat at 4°C.

Imaging.

All confocal images within a dataset were generated with the same confocal microscope with identical laser power and gain settings using NIS-Elements AR software 5.20.02 (RRID:SCR_014329). Images of PV;eGFP tissue were taken with a Nikon A1 inverted LUNV microscope (RRID:SCR_020318) using a 20X water objective and galvanometric scanner (NA 0.95, pixel size: 0.63 μm, field of view: 500×500×13 μm in the XYZ plane with a 0.7 μm step through the z-axis). Images of SST;eGFP tissue were taken with a Nikon AXR Upright microscope using a 25X silicone objective and resonant scanner (NA 1.05, pixel size: 0.5 μm, field of view: 500×500×13 μm in the XYZ plane with a 0.7 μm step). Images taken with the resonant scanner were denoised using NIS-Elements Denoise.ai.

Image collection focused on the hippocampal subregions containing the largest populations of PV+ and SST+ interneurons, including *stratum pyramidale* (PYR) and *stratum oriens* (SO) in CA1 and CA3 and the dentate granule cell body layer and hilus in the dentate. One standardized field of view was obtained to capture PYR and SO in CA1 and CA3. Images of the dentate gyrus were collected with the same imaging parameters, but with a stitched tile scan to encompass the entire dentate granule cell body layer and hilus. For total hippocampal subregion counts, the cell layers were binned for each subregion. For each region of interest, 2–4 confocal images were collected from independent coronal slices from each mouse. Dorsal hippocampal sections were collected between −1.00 to −2.00 mm and ventral hippocampus sections collected between −3.00 to −4.00 mm posterior to bregma in the Allen Mouse Brain Atlas (2004) (RRID:SCR_002978).

Image Quantification.

To evaluate the efficacy of endogenous eGFP in identifying interneurons by antibody immunoreactivity (either PV or SST), we determined sensitivity and specificity for each mouse line. For sensitivity, the number of neurons co-expressing eGFP and either PV or SST was divided by the total number of PV- or SST- immunopositive interneurons. For specificity, the number of neurons co-expressing eGFP and either PV or SST was divided by the total number of eGFP-expressing cells. For these analyses, Imaris 9.7.2 (Oxford Instruments, RRID: SCR_007370) was used to generate spots and assess colocalization (average spot diameter: 15μm). For each region of interest, 2–4 confocal images were analyzed by two blinded observers from independent coronal slices for each mouse. Flippase-negative litter-mate controls lacked eGFP throughout the brain (Figure 1A–B).

To determine the proportion of interneurons which express GR, we used a masked analysis in Imaris to quantify mean fluorescence intensity of GR immunolabeling within eGFP-positive neurons. The threshold for a GR-positive cell was set at twice the average background in the GR channel among the GR-negative neuropil in no primary control (secondary-only) slides (Figure 1B–C). To define cell layers within a hippocampal

subregion, a volume surface projection was created by tracing regions of interest (ROIs) in Imaris. In CA1 and CA3, two ROIs were drawn around the *stratum pyramidale* (PYR) and *stratum oriens* (SO), whereas in the dentate gyrus two ROIs were drawn around the dentate granule cell body layer (DGC-L) and hilus (H). Results are reported as the percentage of total interneurons which are positive for GR ± SEM.

Stereotaxic Viral Injection.

Adult male GR$^{fl/fl}$ or GR$^{wt/wt}$ mice (25–27g) underwent bilateral stereotaxic injection of 3.5e9 viral particles per hemisphere (1 μL of 3.5e11 GC/mL diluted in sterile 1XPBS, pH 7.4) of AAV9.CamKII-Cre-mCherry (Vector Builder). Briefly, mice were anesthetized with isoflurane, shaved, and transferred to a KOPF stereotaxic frame with a nose cone to supply continuous isoflurane (0.5–1.5% at 0.5–1.0 L/min O$_2$). A 2–3 cm sagittal incision was made along the scalp to expose the skull. Two 1 mm holes were drilled through the skull over the hippocampus, leaving the dura mater intact. The needle of a 5 μL Hamilton syringe was lowered slowly into the dentate gyrus of the ventral hippocampus (AP: −3.1, ML: ±3.0, DV: −3.0 mm) and virus was infused at a rate of 200 nL/min. After the needle was withdrawn, holes were filled with bone wax and the scalp was closed with absorbable sutures, Gluture and treated with triple antibiotic. Mice were given carprofen (1 mg/kg, i.p.) and supportive saline for 48 hrs post-surgery and singly-housed with two types of enrichment (nestlet and crinkle paper) until sacrifice.

Statistical Analysis.

All datasets were assessed for normality using the Shapiro-Wilk test in SigmaPlot 14.0 (RRID: SCR_003210). Normally distributed data were analyzed by two-way repeated measures ANOVA with hippocampal subregion (i.e., dentate gyrus, CA1, CA3) and dorsoventral level as factors. To assess cell layer differences within a subregion (e.g. SO vs PYR within CA1), normally distributed data were analyzed by individual paired Student's t tests and non-normal data were analyzed by Mann-Whitney Rank Sum test. Alpha was set at 0.05 and data are presented as mean±SEM.

Figure Preparation.

Graphs were created in GraphPad Prism 9.1.1 (RRID: SCR_002798). Representative micrographs were cropped and adjusted for contrast and brightness using NIS-Elements AR 5.20.02 (RRID:SCR_014329) and Adobe Photoshop CS9 22.5.1 (RRID:SCR_014199). Identical adjustments were made to all images meant for comparison. The graphical abstract was created in Adobe Illustrator 25.4.1 (RRID:SCR_010279).

RESULTS

PV;eGFP and SST;eGFP transgenic mouse lines provide sensitive and specific labeling of respective interneuron populations

The goal of the present study was to determine whether PV- and/or SST-expressing hippocampal interneurons co-express GR. To characterize GR expression among PV and SST interneurons, an approach was developed utilizing transgenic mouse reporter lines. Mice with a FRT-flanked STOP cassette upstream of eGFP (Sousa et al., 2009) were

crossed to PV- (Madisen et al., 2015) or SST-specific (He et al., 2016) flippase-expressing lines to generate: 1) PV;eGFP (PV FlpO$^{+/-}$; Frt-eGFP$^{+/-}$) and 2) SST;eGFP (SST FlpO$^{+/-}$; Frt-eGFP$^{+/-}$) reporters.

To evaluate the efficacy of the flippase-dependent eGFP reporter lines, sections from PV;eGFP and SST;eGFP mice were stained for PV and SST, respectively (Figures 2 and 3). We quantified labeling sensitivity (eGFP+marker+/total marker+) and specificity (eGFP+marker+/total eGFP+) for each mouse line within three hippocampal subregions: CA1, CA3 and the dentate gyrus. Because the dorsal and ventral hippocampus hold unique functions regarding the stress axis, we assessed the two regions independently (Floriou-Servou et al., 2018).

Immunostaining of PV;eGFP tissue revealed high rates of overlap between PV and eGFP signal throughout the hippocampus (Figure 2). Overall, dorsal and ventral areas of the hippocampal subregions did not differ in labeling sensitivity (Figure 2B) (no main effect of dorsoventral level [F(1,23) = 2.611, p =0.205]). The sensitivity of eGFP for detecting PV interneurons (eGFP+PV+/all PV+) by hippocampal subregion was 85.5±0.5% within CA1, 90.5±2.7% within CA3, and 89.2±4.2% within the dentate (Figure 2B) (no main effect of subregion [F(2,23) = 0.652, p =0.554]). Furthermore, eGFP expression was a highly specific marker for PV-immunolabeled interneurons (eGFP+PV+/all eGFP+), regardless of dorsoventral level, with 91.1± 2.5% of eGFP+ cells staining for PV in CA1, 82.0±1.0% in CA3, and 79.5±3.3% in the DG (Figure 2C) (no main effect of dorsoventral level [F(1,23) = 0.0115, p =0.921]). Although a two-way repeated measures ANOVA suggested a main effect of cell layer (main effect of cell layer [F(2,23) = 5.342, p= 0.047, *post-hoc* p = 0.063]), with mean specificity in CA1 trending higher than in the dentate, Bonferroni *post-hoc* pairwise comparison revealed no significant differences in regional specificity. Therefore, we cautiously conclude that specificity of eGFP for PV+ interneurons did not vary across hippocampal subregions (Figure 2C).

Immunostaining of SST;eGFP tissue also revealed high levels of co-labeling between SST and eGFP among the three hippocampal subregions across the dorsal and ventral hippocampus (Figure 3). The sensitivity of eGFP for detecting SST+ interneurons (eGFP+SST+/all SST+) by hippocampal subregion was 91.4±3.2% within CA1, 78.3±11.1% within CA3, and 76.7±6.4% within the dentate (Figure 3B) (no main effect of cell layer [F(2,23) = 1.847, p = 0.270]). Similarly, eGFP provided a highly specific marker for SST interneurons (eGFP+SST+/all eGFP+), with 90.2±2.5% in CA1, 77.9±6.6% in CA3, and 75.5±7.4% in the dentate (Figure 3C) (no main effect of cell layer [F(2,23) = 3.678, p = 0.124]). Taken together, these data support the use of PV;eGFP and SST;eGFP transgenic reporter mouse lines to accurately and robustly label the respective interneuron populations with high sensitivity and specificity.

Hippocampal PV+ interneuron GR expression depends on hippocampal subregion and cell layer

To determine whether PV+ hippocampal interneurons could be direct targets for corticosteroid action, tissue from PV;eGFP mice was immunostained for GRs. Putative PV+ interneurons were identified by eGFP+ expression within dorsal and ventral CA1, CA3 and

dentate. For these analyses, the hippocampal layers containing the largest populations of PV+ interneurons were examined independently. In CA1 and CA3, GR co-expression was quantified within the *stratum pyramidale* (PYR) and *stratum oriens* (SO). In the dentate gyrus, quantification was conducted in the dentate hilus (H) and the dentate granule cell body layer (DGC-L).

Hippocampal PV+ interneuron GR expression was heterogeneous depending on subregion (CA1, CA3, vs dentate), cell layer (SO vs PYR) and dorsoventral level (dorsal vs ventral) (Figure 4). Aggregated dorsoventral data revealed the highest percentage of GR co-expression among CA3 PV+ interneurons, at $78.2 \pm 8.2\%$ (main effect of subregion $[F(2,23) = 6.016$, *post hoc* $p = 0.003]$) compared to both CA1 PV+ interneurons ($55.6 \pm 6.5\%$) and the dentate gyrus ($69.5 \pm 7.3\%$) (Figure 4B) (main effect of subregion $[F(2,23) = 4.606$, *post hoc* $p = 0.011]$).

Within CA1 and CA3, GR expression did not differ between dorsal and ventral hippocampus (Figure 4B) (no main effect of CA1 dorsoventral level $[F(1,23) = 0.0674$, *post hoc* $p = 0.948]$; no main effect of CA3 dorsoventral level $[F(1,23) = 0.204$, *post hoc* $p = 0.843]$). However, among the cell layers of CA1 and CA3, a higher percentage of PV+ interneurons in the *stratum pyramidale* expressed GR compared to cells in the adjacent *stratum oriens* (Figure 4C) (CA1: $t(30) = -5.677$, $p < 0.001$; CA3: Mann-Whitney $U = 30.0$, $n_1 = n_2 = 20$, $p < 0.001$).

The dentate gyrus exhibited a unique GR expression pattern compared to CA1 and CA3. We found an interesting dorsoventral variation in GR expression, with a smaller proportion of PV+ interneurons expressing GR in the ventral ($50.9 \pm 6.8\%$) compared to the dorsal ($88.2 \pm 7.9\%$) dentate (Figure 4B) (main effect of dorsoventral level $[F(1,23) = 2.844$, *post hoc* $p = 0.019]$). In contrast to CA1 and CA3, there were no cell-layer specific differences in PV+ interneuron GR expression between the hilus and dentate granule cell layer (Figure 4C).

Taken together, these data suggest that baseline GR expression in hippocampal PV+ interneurons is heterogeneous depending on cell layer, subregion and dorsoventral level. This variability in GR expression implies divergent functional responses to glucocorticoids among different parts of the PV+ inhibitory neural network of the hippocampus.

Hippocampal SST+ interneuron GR expression is ubiquitous

SST+ hippocampal interneurons are positioned to coordinate complex inhibitory interconnections and tightly modulate hippocampal microcircuitry. In contrast to PV+ interneurons, GR immunostaining of SST;eGFP tissue across dorsal and ventral CA1, CA3 and dentate cell layers revealed ubiquitous expression compared to PV+ interneurons. We detected near-100% co-expression of GR and SST+ across the hippocampus (Figure 5B) (no main effect of dorsoventral level $[F(1,17)=3.994$, $p = 0.184]$, no main effect of subregion $[F(2,17)=1.575$, $p = 0.313]$). Further, subregional analysis revealed similarly high GR expression among the *stratum pyramidale* and *stratum oriens* of CA1 and CA3 as well as within the dentate hilus and granule cell layer (Figure 5C).

Taken together, these data suggest hippocampal SST+ interneurons are putative direct targets for serum glucocorticoids via GR-mediated signaling regardless of positioning in hippocampal subregion, sublayer and dorsoventral level.

Viral-mediated GR deletion confirms biological specificity of GR immunostaining

To confirm the biological selectivity of the GR antibody used in these studies, we immunostained tissue from adult male GR$^{fl/fl}$ (knockout) and GR$^{wt/wt}$ (control) mice following hippocampal injection of AAV9.CaMKII-Cre-mCherry (Figure 6A). The viral construct leads to deletion of GR from forebrain excitatory neurons and simultaneous expression of mCherry. GR immunostaining in knockout conditions revealed a marked absence of GR immunoreactivity among mCherry positive dentate granule cells relative to adjacent mCherry negative cells, while GR immunoreactivity was unaffected in controls regardless of mCherry expression (Figure 6B). This genetic approach confirms the biological selectivity of the GR primary antibody used throughout this study.

DISCUSSION

While stress hormone receptor expression among hippocampal glutamatergic neurons has been well-characterized, neighboring interneuron receptor expression has been relatively unexplored. Here, we combined eGFP reporter mouse lines with GR immunochemistry to assess GR co-expression among PV+ and SST+ interneurons. We found a heterogeneous pattern of GR expression, depending on interneuron type and hippocampal subregion. Almost all SST+ interneurons were GR immunopositive, whereas PV+ interneuron GR expression varied across hippocampal subregion and cell layer. Thus, PV+ and SST+ hippocampal interneurons represent putative direct glucocorticoid targets and the heterogeneous pattern of GR expression suggests a cell type- and region-specific response.

Utility of eGFP-flippase transgenic mouse lines for interneuron identification

Studies utilized flippase-dependent double transgenic eGFP reporter lines (PV$^{+/-}$;eGFP$^{+/-}$ and SST$^{+/-}$;eGFP$^{+/-}$) to label PV+ and SST+ hippocampal interneurons, respectively. Compared to interneuron identification by immunohistochemistry, this approach has relative advantages and disadvantages. Advantages include the ease of detecting eGFP labeling (enhanced sensitivity) and the elimination of potential antibody cross-reactivity. Conversely, insertion of the transgene can alter endogenous promotor activity and reduce labeling fidelity. Further, transient promoter/Cre recombinase activity will lead to permanent eGFP expression. Because interneuron marker expression can change over the course of development (Pelkey et al., 2017), eGFP labeling may not align with PV or SST protein levels at the time of sacrifice. Consistent with these caveats, correspondence between eGFP and PV/SST immunoreactivity did not reach 100%. We note, however, that immunohistochemical approaches also produce false positives and negatives, so additional cell-identification approaches (e.g., single cell RNA sequencing) are required to corroborate our findings. Importantly, morphological examination supports the efficacy of the transgenic labeling approach within the hippocampus, as eGFP+ cells were present in the expected location and frequency with interneuron-like morphology.

Multifactorial interneuron response to glucocorticoids

The present study reveals that a substantial population of hippocampal interneurons express GR, a ligand-binding transcription factor that translocates to the nucleus upon glucocorticoid binding. GR signaling occurs in conjunction with activation of mineralocorticoid receptors (MRs), which also bind glucocorticoids, albeit with higher affinity (De Kloet, 2014). Together, the dynamic balance between MR- and GR-activation controls cell- and circuit-level activation by the hormonal stress response (De Kloet et al., 1998; Harris et al., 2013). In addition, GR can act at or near the cell membrane to exert fast non-genomic modulation of cellular excitability (Scheschowitsch et al., 2017). Among excitatory hippocampal cells, exposure to GR-specific agonists can affect neuronal excitability, resulting in an initial excitatory response that gives way to a more prolonged inhibition (De Kloet, 2014). Whether these direct effects hold true for interneurons remains unknown; however, glucocorticoid exposure has been shown to enhance interneuron function *indirectly* by promoting nitric oxide release from GR-expressing pyramidal neurons (Hu et al., 2010).

In addition to GR and MR, hippocampal interneurons also express corticotropin-releasing hormone (CRH), another key regulator of stress signaling. CRH is locally synthesized in the hippocampus and released in response to stress (Chen et al., 2004, 2012; Yan et al., 1998). Interestingly, CRH is expressed in interneurons whose somata are located within the pyramidal cell layers of CA1 and CA3, such as PV+ basket and chandelier cells (Yan et al., 1998). Once released, CRH acts at its receptor among the dendrites of pyramidal neurons to impact synaptic function in a time-and dose-dependent manner (Chen et al., 2012). Thus, establishing the functional consequence of glucocorticoid exposure among hippocampal interneurons requires electrophysiological studies and understanding the multifactorial response dependent on MR:GR balance, local CRH release and both direct and indirect effects of receptor activation.

Patterns of hippocampal GR expression

Protein and mRNA studies have revealed high expression of GR *(Nr3c1)* among the glutamatergic neurons of CA1, CA2, the dentate gyrus, and moderate expression in CA3 (Herman, 1993; Wang et al., 2013). In contrast, interneuron-specific expression data for *Nr3c1* is limited. Recently, Viho and colleagues utilized single cell RNA- sequencing data to correlate *Nr3c1* levels with the expression of interneuron-specific markers in the mouse hippocampus (Viho et al., 2021). They found that ~60% of hippocampal neurons expressing PV mRNA co-expressed *Nr3c1* - aligning well with the present study - but only ~35% of cells expressing SST mRNA co-expressed *Nr3c1.* Several variables could account for the discrepancy. Firstly, we note that mRNA and protein assays have appreciable differences in tissue preparation and sensitivity, which may lead to under sampling biases in both techniques. Secondly, mRNA and protein expression can diverge depending on regulation of translation and protein stability. Thirdly, the single cell RNA sequencing data was gathered from whole hippocampal extracts which included regions which were not sampled in the present study: *stratum radiatum* and *lacunosum moleculare.* It remains possible that SST+ interneurons within these regions do not express GR or that differences in internal and external conditions affected GR expression among these neurons.

Variable expression of GRs among parvalbumin+ interneurons

In the hippocampus, PV+ interneurons are found throughout the cell layers of CA1, CA3 and the dentate gyrus. In CA1 and CA3, we analyzed GR expression among PV+ interneurons of the *stratum pyramidale* and *oriens,* likely consisting of basket cells, axo-axonic cells and bistratified dendritic interneurons. Basket cells and axo-axonic cells exert tight control over pyramidal cell firing, with fast-spiking trains of action potentials directed to somata, proximal dendrites and axon initial segments (Cobb et al., 1995). Approximately half of PV+ bistratified dendritic interneurons of the *stratum oriens* co-express SST (Booker & Vida, 2018); therefore, this cell type was likely represented in both PV+ and SST+ datasets, and as such, likely expresses GR. PV+, SST+ bistratified dendritic interneurons exert most of their influence on a single cell layer, providing highly controlled pathway-specific inhibition (Melzer et al., 2012). Because the somata of all three PV+ cell types are dispersed throughout the *stratum radiatum* and *oriens* of CA1 and CA3, GR expression among PV+ cells does not appear to correspond to a specific interneuron subtype; rather, GR expression levels may represent an additional criterion by which to categorize hippocampal PV+ interneurons. Alternatively, GR expression may fluctuate over time and condition within the PV+ interneuron population, as has been demonstrated for PV+ interneurons in the medial prefrontal cortex following exposure of rodents to chronic stress (McKlveen et al., 2016). Future studies should probe whether a static proportion of PV+ hippocampal interneurons remain refractory to GR signaling or whether these cells dynamically regulate GR expression.

GR expression in PV+ interneurons was enriched in the CA3 pyramidal cell layer, with relatively lower expression in CA1 and the dentate gyrus. This is the inverse of the generally accepted pattern of GR expression among the corresponding hippocampal excitatory neurons, suggesting cell- and subregion-specific modulation of GR expression. In the dentate, there were no differences in GR expression between PV+ interneurons in the hilus versus those in the dentate granule cell layer. Notably, PV+ interneurons in the dorsal dentate gyrus were enriched for GR expression compared to the ventral dentate. This may reflect the more active role that the ventral hippocampus plays in HPA axis regulation. Further studies are necessary to understand the functional consequences of PV+ GR expression relative to surrounding pyramidal cells.

Ubiquitous expression of GRs in somatostatin+ interneurons

In general, SST+ interneurons with both short- and long-range projections tend to function as modulators, with more tempered control over pyramidal cell membrane potential through regular-spiking trains of action potentials directed at distal dendritic synapses (Buhl et al., 1994). In contrast to PV, we found near 100% expression of GR among the SST+ interneurons assessed within CAI, CA3 and dentate gyrus. With ubiquitous GR expression, we do not expect GR immunoreactivity to define further subdivisions of SST+ interneurons based on stress-dependent signaling.

Sexual dimorphism in GR expression and regulation

In prior studies, targeted knockdown of GRs from various forebrain interneuron populations altered HPA axis excitability and avoidance behavior specifically in females (McKlveen

et al., 2013; Scheimann et al., 2018, 2019). In addition, *Nr3c1* is co-expressed with sex-specific steroid receptor mRNA in interneurons of the hippocampus (Viho et al. 2021). While no sex differences were found in the present study (data not shown), group sizes for this analysis were small and the absence of effects should be interpreted with caution.

Conclusions

The present study demonstrates that almost all hippocampal SST+ interneurons and the majority PV+ interneurons are GR immunopositive under non-stressed, morning diurnal conditions. Our findings indicate that these interneurons represent putative direct targets for glucocorticoid action. As such, HPA axis dysregulation and associated hyper-or hypo-cortisolemia - conditions frequently associated with neurological disorders - could directly disrupt interneuron function. Conversely, interneuron loss, as in epilepsy, likely removes key components of the HPA axis, perhaps contributing to dysregulation that is common to the disease (Kanner, 2011). Thus, the conclusions from this study provide a starting point to better understand how hippocampal inhibitory circuitry might respond to glucocorticoid exposure, information crucial to understanding the mechanisms of HPA axis dysregulation across disease states.

REFERENCES

Allen Reference Atlas - Mouse Brain [coronal]. Available from atlas.brain-map.org.

Booker SA, & Vida I. (2018). Morphological diversity and connectivity of hippocampal interneurons. Cell and Tissue Research, 373, 619–641. 10.1007/s00441-018-2882-2 [PubMed: 30084021]

Buhl EH, Halasy K, & Somogyi P. (1994). Diverse sources of hippocampal unitary inhibitory postsynaptic potentials and the number of synaptic release sites. Nature, 368, 823–828. 10.1038/368823a0 [PubMed: 8159242]

Carroll BJ, Curtis GC, & Mendels J. (1976). Neuroendocrine regulation in depression: Limbic system-adrenocortical dysfunction. Archives of General Psychiatry, 33(9), 1039–1044.10.1001/archpsyc.1976.01770090029002 [PubMed: 962488]

Castro OW, Santos VR, Pun RYK, McKlveen JM, Batie M, Holland KD, Gardner M, Garcia-Cairasco N, Herman JP, & Danzer SC (2012). Impact of corticosterone treatment on spontaneous seizure frequency and epileptiform activity in mice with chronic epilepsy. PLoS ONE, 7(9), e46044. 10.1371/journal.pone.0046044

Chen Y, Andres AL, Frotscher M, & Baram TZ (2012). Tuning synaptic transmission in the hippocampus by stress: The CRH system. Frontiers in Cellular Neuroscience, 6(APRIL 2012), 1–7. 10.3389/fncel.2012.00013 [PubMed: 22319471]

Chen Y, Brunson KL, Adelmann G, Bender RA, Frotscher M, & Baram TZ (2004). Hippocampal corticotropin releasing hormone: Pre- and postsynaptic location and release by stress. Neuroscience, 126(3), 533–540. 10.1016/j.neuroscience.2004.03.036 [PubMed: 15183503]

Cobb SR, Buhl EH, Halasy K, Paulsen O, & Somogyi P. (1995). Synchronization of neuronal activity in hippocampus by individual GABAergic interneurons. Nature, 378, 75–78. 10.1038/378075a0 [PubMed: 7477292]

De Kloet ER (2014). From receptor balance to rational glucocorticoid therapy. Endocrinology, 155(8), 2754–2769. 10.1210/en.2014-1048 [PubMed: 24828611]

De Kloet ER, Vreugdenhil E, Oitzl MS, & Joels M. (1998). Brain corticosteroid receptor balance in health and disease. Endocrine Reviews, 19(3), 269–301. 10.1210/er.19.3.269 [PubMed: 9626555]

Dieleman GC, Huizink AC, Tulen JHM, Utens EMWJ, Creemers HE, van der Ende J, & Verhulst FC (2015). Alterations in HPA-axis and autonomic nervous system functioning in childhood anxiety disorders point to a chronic stress hypothesis. Psychoneuroendocrinology, 51, 135–150. 10.1016/j.psyneuen.2014.09.002 [PubMed: 25305548]

Dunn JD, & Orr SE (1984). Differential plasma corticosterone responses to hippocampal stimulation. Experimental Brain Research, 54, 1–6. 10.1007/BF00235813 [PubMed: 6321219]

Erhardt A, Ising M, Unschuld PG, Kern N, Lucae S, Pütz B, Uhr M, Binder EB, Holsboer F, & Keck ME (2006). Regulation of the hypothalamic-pituitary- adrenocortical system in patients with panic disorder. Neuropsychopharmacology, 31, 2515–2522. 10.1038/sj.npp.1301168 [PubMed: 16841071]

Floriou-Servou A, von Ziegler L, Stalder L, Sturman O, Privitera M, Rassi A, Cremonesi A, Thony B, & Bohacek J. (2018). Distinct proteomic, transcriptomic, and epigenetic stress responses in dorsal and ventral hippocampus. Biological Psychiatry, 84(7), 531–541. 10.1016/j.biopsych.2018.02.003 [PubMed: 29605177]

Harris AP, Holmes MC, De Kloet ER, Chapman KE, & Seckl JR (2013). Mineralocorticoid and glucocorticoid receptor balance in control of HPA axis and behaviour. Psychoneuroendocrinology, 38(5), 648–658. 10.1016/j.psyneuen.2012.08.007 [PubMed: 22980941]

He M, Tucciarone J, Lee SH, Nigro MJ, Kim Y, Levine JM, Kelly SM, Krugikov I, Wu P, Chen Y, Gong L, Hou Y, Osten P, Rudy B, & Huang ZJ (2016). Strategies and tools for combinatorial targeting of GABAergic neurons in mouse cerebral cortex. Neuron, 91(6), 1228–1243. 10.1016/Zj.neuron.2016.08.021 [PubMed: 27618674]

Herman JP (1993). Regulation of adrenocorticosteroid receptor mRNA expression in the central nervous system. Cellular and Molecular Neurobiology, 13, 349–372. 10.1007/BF00711577 [PubMed: 8252607]

Herman JP, Figueiredo H, Mueller NK, Ulrich-lai Y, Ostrander MM, Choi DC, & Cullinan WE (2003). Central mechanisms of stress integration: hierarchical circuitry controlling hypothalamo-pituitary- adrenocortical responsiveness. Frontiers in Neuroendocrinology, 24(3), 151–180. 10.1016/j.yfrne.2003.07.001 [PubMed: 14596810]

Herman JP, & Mueller NK (2006). Role of the ventral subiculum in stress integration. Behavioural Brain Research, 174, 215–224. 10.1016/j.bbr.2006.05.035 [PubMed: 16876265]

Herman JP, Schafer MKH, Young EA, Thompson R, Douglass J, Akil H, & Watson SJ (1989). Evidence for hippocampal regulation of neuroendocrine neurons of the hypothalamo-pituitary-adrenocorticoid axis. Journal of Neuroscience, 9(9), 3072–3082. 10.1523/jneurosci.09-09-03072.1989 [PubMed: 2795152]

Hu W, Zhang M, Czeh B, Flügge G, & Zhang W. (2010). Stress impairs GABAergic network function in the hippocampus by activating nongenomic glucocorticoid receptors and affecting the integrity of the parvalbumin-expressing neuronal network. Neuropsychopharmacology, 35(8), 1693–1707. 10.1038/npp.2010.31 [PubMed: 20357756]

Joels M. (2009). Stress, the hippocampus, and epilepsy. Epilepsia, 50(4), 586–597. 10.1111/j.1528-1167.2008.01902.x [PubMed: 19054412]

Kanner AM (2011). Depression and epilepsy: A bidirectional relation? Epilepsia, 52(Suppl 1), 21–27. 10.1111/j.1528-1167.2010.02907.x

Madisen L, Garner AR, Shimaoka D, Chuong AS, Klapoetke NC, Li L, van der Bourg A, Niino Y, Egolf L, Monetti C, Gu H, Mills M, Cheng A, Tasic B, Nguyen TN, Sunkin SM, Benucci A, Nagy A, Miyawaki A, … Zeng H. (2015). Transgenic mice for intersectional targeting of neural sensors and effectors with high specificity and performance. Neuron, 85(5), 942–958. 10.1016/j.neuron.2015.02.022 [PubMed: 25741722]

McKlveen JM, Morano RL, Fitzgerald M, Zoubovsky S, Cassella SN, Scheimann JR, Ghosal S, Mahbod P, Packard BA, Myers B, Baccei ML, & Herman JP (2016). Chronic stress increases prefrontal inhibition: a mechanism for stress-induced prefrontal dysfunction. Biological Psychiatry, 80(10), 754–764. 10.1016/j.biopsych.2016.03.2101 [PubMed: 27241140]

McKlveen JM, Myers B, Flak JN, Bundzikova J, Solomon MB, Seroogy KB, & Herman JP (2013). Role of prefrontal cortex glucocorticoid receptors in stress and emotion. Biological Psychiatry, 74(9), 672–679. 10.1016/j.biopsych.2013.03.024 [PubMed: 23683655]

Melzer S, Michael M, Caputi A, Eliava M, Fuchs EC, Whittington MA, & Monyer H. (2012). Long-range-projecting gabaergic neurons modulate inhibition in hippocampus and entorhinal cortex. Science, 335(6075), 1506–1510. 10.1126/science.1217139 [PubMed: 22442486]

Olijslagers JE, De Kloet ER, Elgersma Y, Van Woerden GM, Joels M, & Karst H. (2008). Rapid changes in hippocampal CA1 pyramidal cell function via pre- as well as postsynaptic membrane mineralocorticoid receptors. European Journal of Neuroscience, 27(10), 2542–2550. 10.1111/Zj.1460-9568.2008.06220.x [PubMed: 18547242]

Pasricha N, Joels M, & Karst H. (2011). Rapid effects of corticosterone in the mouse dentate gyrus via a nongenomic pathway. Journal of Neuroendocrinology, 23, 143–147. 10.1111/j.1365-2826.2010.02091.x [PubMed: 21092068]

Pelkey KA, Chittajallu R, Craig MT, Tricoire L, Wester JC, & McBain CJ (2017). Hippocampal gabaergic inhibitory interneurons. Physiological Reviews, 97,1619–1747. 10.1152/physrev.00007.2017 [PubMed: 28954853]

Radley JJ, & Sawchenko PE (2011). A common substrate for prefrontal and hippocampal inhibition of the neuroendocrine stress response. Journal of Neuroscience, 31(26), 9683–9695. 10.1523/JNEUR0SCI.6040-10.2011 [PubMed: 21715634]

Rubin RT, Mandell AJ, & Crandall PH (1966). Corticosteroid responses to limbic stimulation in man: Localization of stimulus sites. Science, 153(3737), 767–768. 10.1126/science.153.3737.767 [PubMed: 5940897]

Scheimann JR, Mahbod P, Morano R, Frantz L, Packard B, Campbell K, & Herman JP (2018). Deletion of glucocorticoid receptors in forebrain GABAergic neurons alters acute stress responding and passive avoidance behavior in female mice. Frontiers in Behavioral Neuroscience, 12(December), 1–10. 10.3389/fnbeh.2018.00325 [PubMed: 29403366]

Scheimann JR, Moloney RD, Mahbod P, Morano RL, Fitzgerald M, Hoskins O, Packard BA, Cotella EM, Hu YC, & Herman JP (2019). Conditional deletion of glucocorticoid receptors in rat brain results in sex- specific deficits in fear and coping behaviors. ELife, 8, e44672. 10.7554/eLife.44672

Scheschowitsch K, Leite JA, & Assreuy J. (2017). New insights in glucocorticoid receptor signaling-more than just a ligand-binding receptor. Frontiers in Endocrinology, 8(16), 19–21. 10.3389/fendo.2017.00016 [PubMed: 28220108]

Sousa VH, Miyoshi G, Hjerling-Leffler J, Karayannis T, & Fishell G. (2009). Characterization of Nkx6–2-derived neocortical interneuron lineages. Cerebral Cortex, 19(1), 1–10. 10.1093/cercor/bhp038 [PubMed: 18448452]

Ulrich-Lai YM, & Herman JP (2009). Neural Regulation of Endocrine and Autonomic Stress Responses. Nat Rev Neurosci, 10(6), 397–409. 10.1038/nrn2647.Neural [PubMed: 19469025]

Van Eekelen JAM, Jiang W, De Kloet ER, & Bohn MC (1988). Distribution of the mineralocorticoid and the glucocorticoid receptor mRNAs in the rat hippocampus. Journal of Neuroscience Research, 1, 88–94. 10.1002/jnr.490210113

Vandevyver S, Dejager L, & Libert C. (2014). Comprehensive overview of the structure and regulation of the glucocorticoid receptor. Endocrine Reviews, 35(4), 671–693. 10.1210/er.2014-1010 [PubMed: 24937701]

Viho EMG, Buurstede JC, Berkhout JB, Mahfouz A, & Meijer OC (2021). Cell type specificity of glucocorticoid signaling in the adult mouse hippocampus. Journal of Neuroendocrinology, November, 1–19. 10.1111/jne.13072

Wang Q, Van Heerikhuize J, Aronica E, Kawata M, Seress L, Joels M, Swaab DF, & Lucassen PJ (2013). Glucocorticoid receptor protein expression in human hippocampus; stability with

age. Neurobiology of Aging, 34(6), 1662–1673. 10.1016/j.neurobiolaging.2012.11.019 [PubMed: 23290588]

Yan XX, Toth Z, Schultz L, Ribak CE, & Baram TZ (1998). Corticotropin- releasing hormone (CRH)-containing neurons in the immature rat hippocampal formation: Light and electron microscopic features and colocalization with glutamate decarboxylase and parvalbumin. Hippocampus, 8(3), 231–243. 10.1002/(SICI)1098-1063(1998)8:3<231::AID-HIPO6>3.0.CO;2-M [PubMed: 9662138]
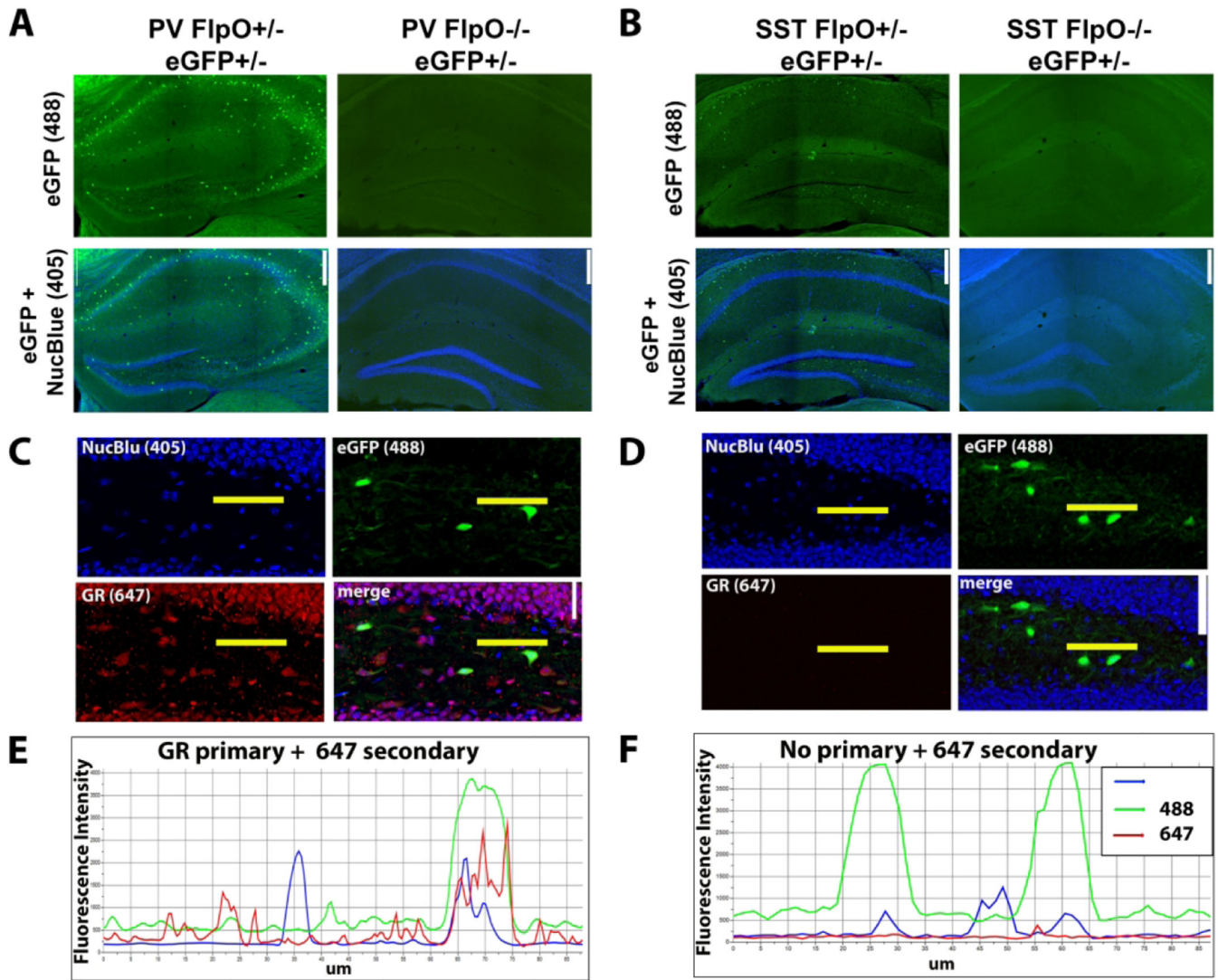
Figure 1. Transgenic labeling of interneurons.

A & B: Flippase-mediated recombination led to robust eGFP (488) labeling of PV **(A)** and SST **(B)** interneurons in the hippocampus, while flippase-negative control mice lacked eGFP expression. Scale bar = 250 μm. **C & D**: Confocal images of dentate gyri in SST-eGFP tissue immunostained with GR antibodies **(C)** and a no-primary control, for which the GR antibody was excluded **(D)**. Scale bar = 25 μm. **E & F:** Fluorescence intensity profiles for 405 (nuclear blue), 488 (eGFP) and 647 (GR) channels along the length (Mm from left to right) of the horizontal yellow lines shown in C and D. GR immunostained tissue shows corresponding peaks for nuclear blue, eGFP and GR immunoreactivity **(E),** while the GR peak (red line) is absent from the no-primary control **(F)**. Fluorescence intensity from no-primary controls was also used to determine background fluorescence and establish a threshold (2x background) for defining GR-positive from GR-negative cells.
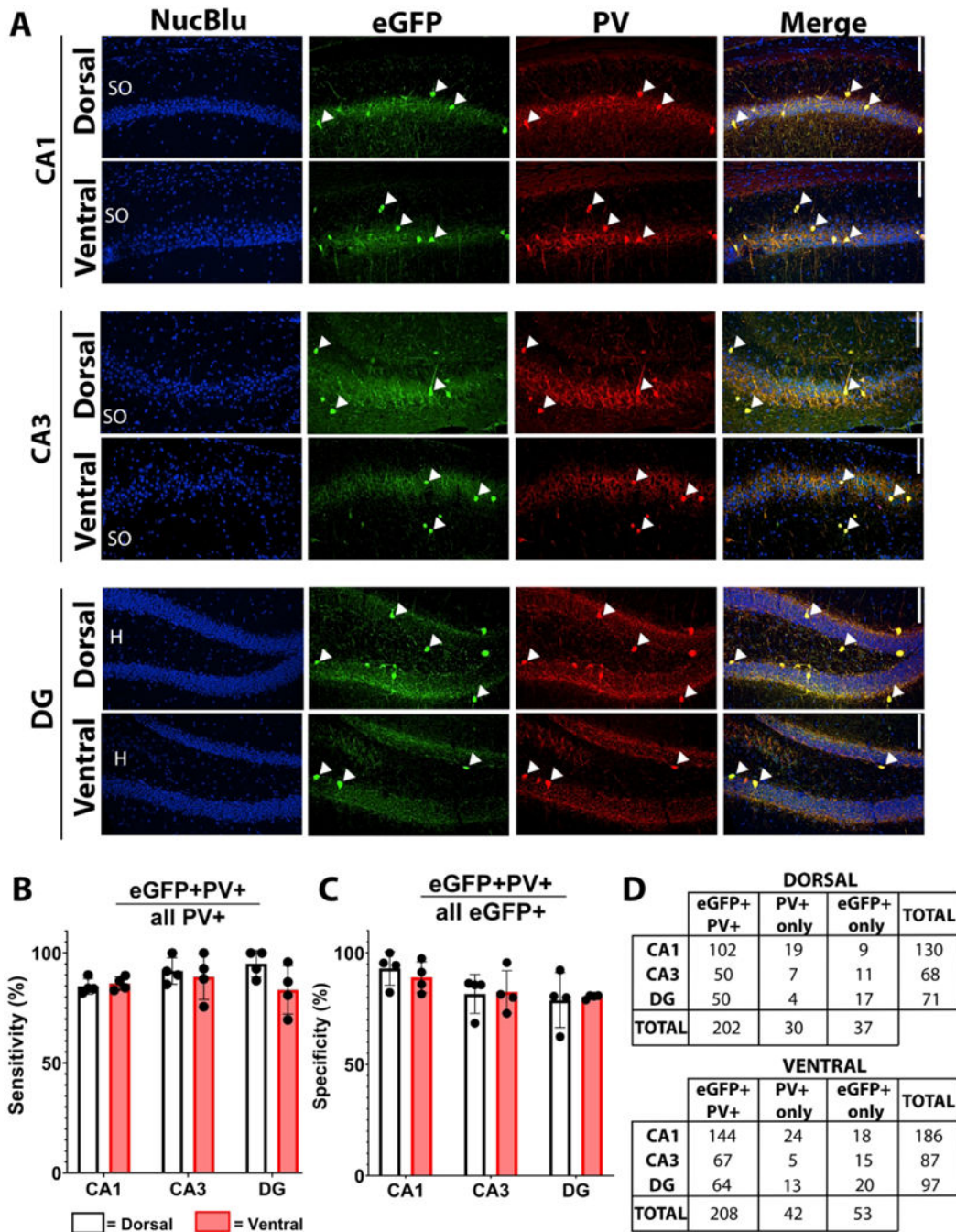
DORSAL

	eGFP+ PV+	PV+ only	eGFP+ only	TOTAL
CA1	102	19	9	130
CA3	50	7	11	68
DG	50	4	17	71
TOTAL	202	30	37	

VENTRAL

	eGFP+ PV+	PV+ only	eGFP+ only	TOTAL
CA1	144	24	18	186
CA3	67	5	15	87
DG	64	13	20	97
TOTAL	208	42	53	

Figure 2. eGFP and PV co-expression in the hippocampus of PV;eGFP reporter mice.
A) Representative micrographs of dorsal and ventral CA1, CA3 and dentate gyrus (DG). Solid arrowheads highlight co-expressing cells throughout the *stratum oriens* (SO), *stratum pyramidale* (PYR), dentate granule cell body layer (DGC-L) and hilus (H). Scale bar = 100 μm. **B)** Sensitivity of eGFP for PV (eGFP+PV+/all PV+). **C)** Specificity of eGFP for PV (eGFP+PV+/all eGFP+). **D)** Cell counts (n) for each condition. Bars represent mean±SEM.
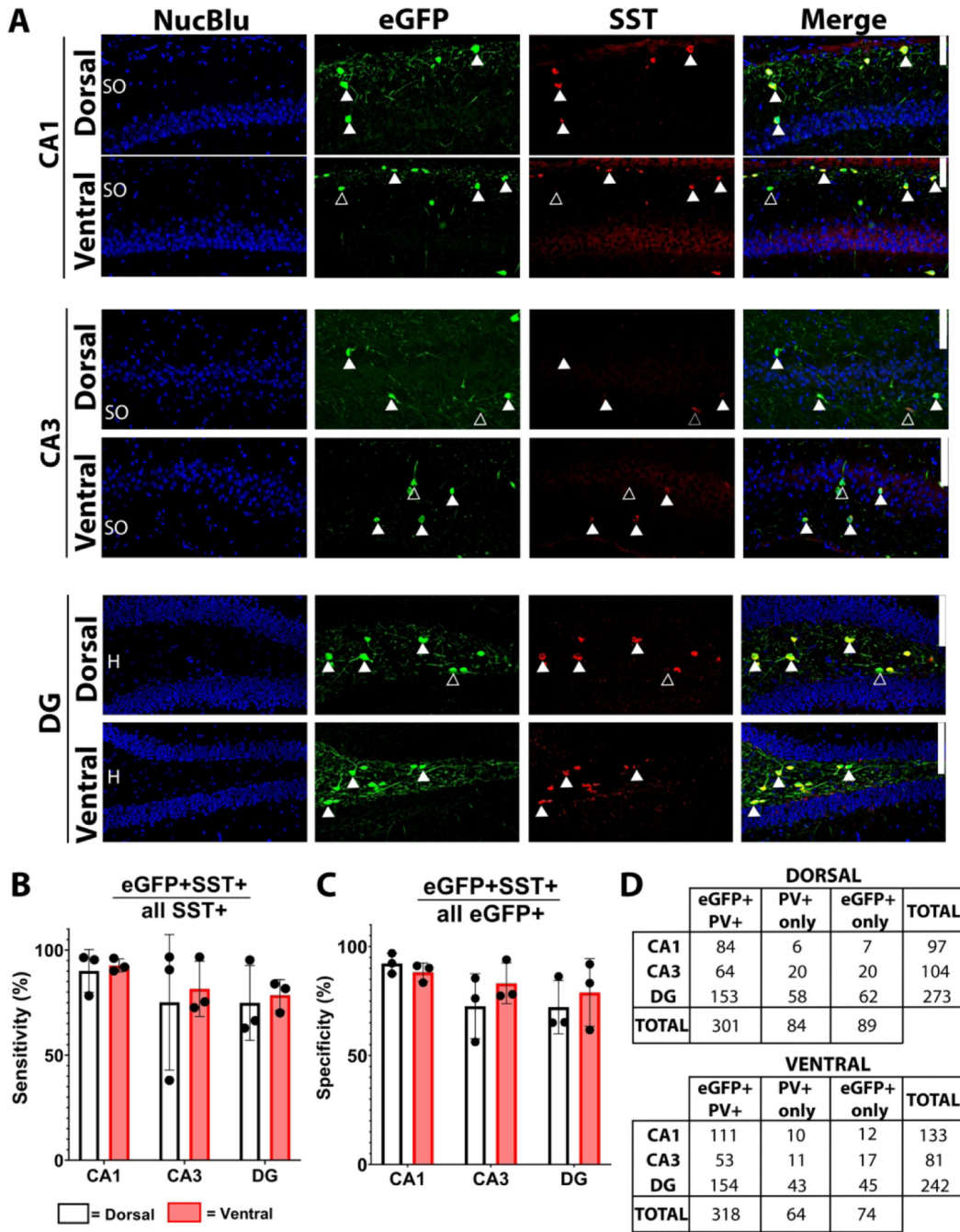
Figure 3. eGFP and SST co-expression in the hippocampus of SST;eGFP reporter mice.
A) Representative micrographs of dorsal and ventral CA1, CA3 and dentate gyrus
(DG). Solid arrowheads highlight co-expressing cells, while empty arrows indicate non-co-
expressing cells throughout the *stratum oriens* (SO), *stratum pyramidale* (PYR), dentate
granule cell body layer (DGC-L) and hilus (H). Scale bar = 100 μm. **B)** Sensitivity of eGFP
for SST (eGFP+SST+/all SST+). **C)** Specificity of eGFP for SST (eGFP+SST+/all eGFP+).
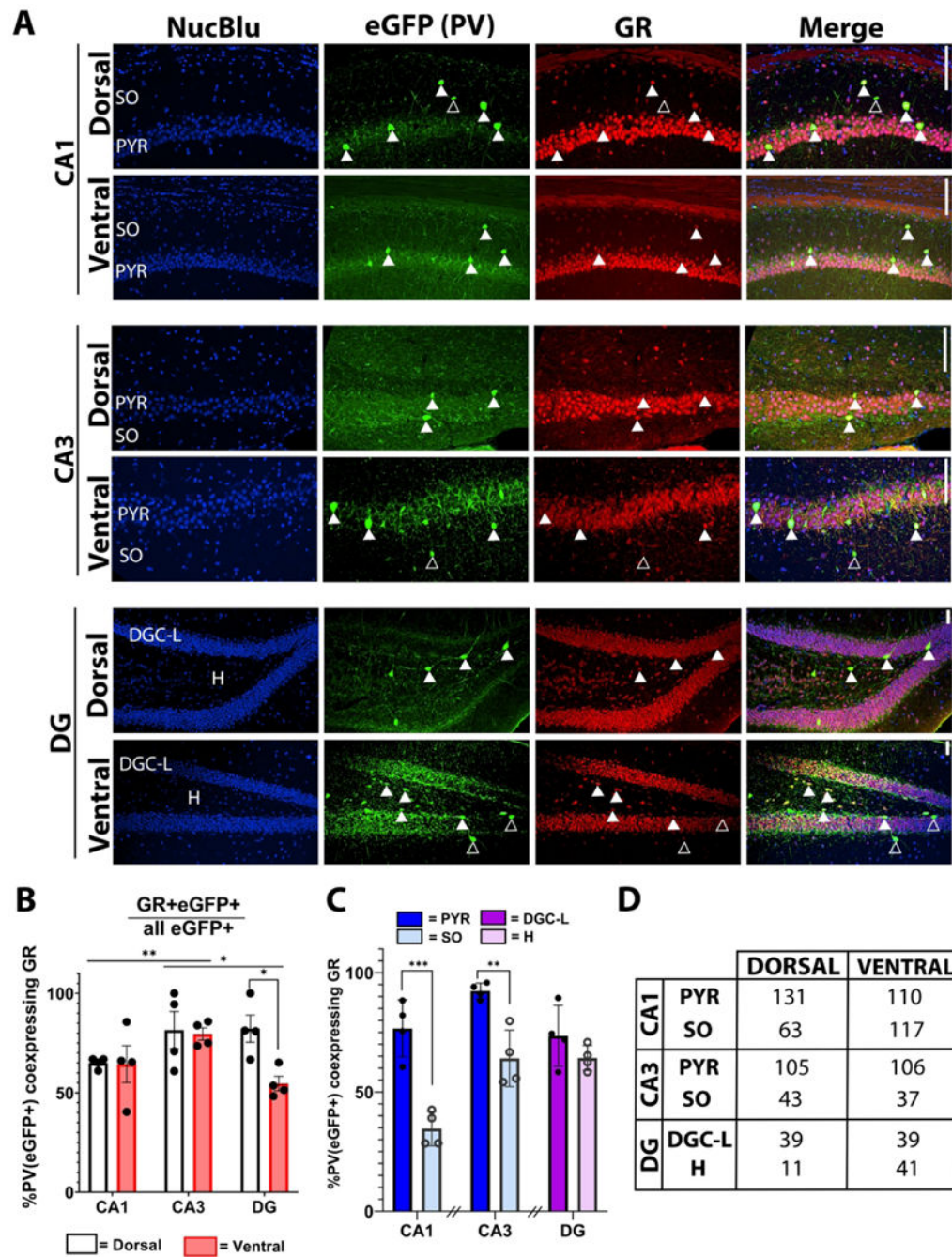**D)** Cell counts (n) for each condition. Bars represent mean±SEM.

Figure 4. Hippocampal PV+ interneuron GR expression is heterogeneous.
A) Representative micrographs of PV+ interneuron GR expression in dorsal and ventral CA1, CA3 and dentate gyrus (DG). Solid arrows highlight co-expressing cells, while empty arrows indicate non-co-expressing cells throughout the *stratum oriens* (SO), *stratum pyramidale* (PYR), dentate granule cell body layer (DGC-L) and hilus (H). Scale bar = 100 μm. **B)** Percentage of PV+ interneurons which express GR by dorsal (white) and ventral (red) hippocampal subregion. *p<0.05, **p<0.01, ***p<0.001, main effect by two-way RM ANOVA with Bonferroni post-hoc pairwise comparison. **C)** Percentage of PV+ interneurons

which express GR, presented by cell layer within CA1, CA3 and DG. **D)** Cell counts (n) for each condition. *p<0.05, **p<0.01, ***p<0.001 by Student's t test or Mann-Whitney Rank Sum test. Breaks in the x-axis indicate groups of data which were not statistically compared. Bars represent mean±SEM.
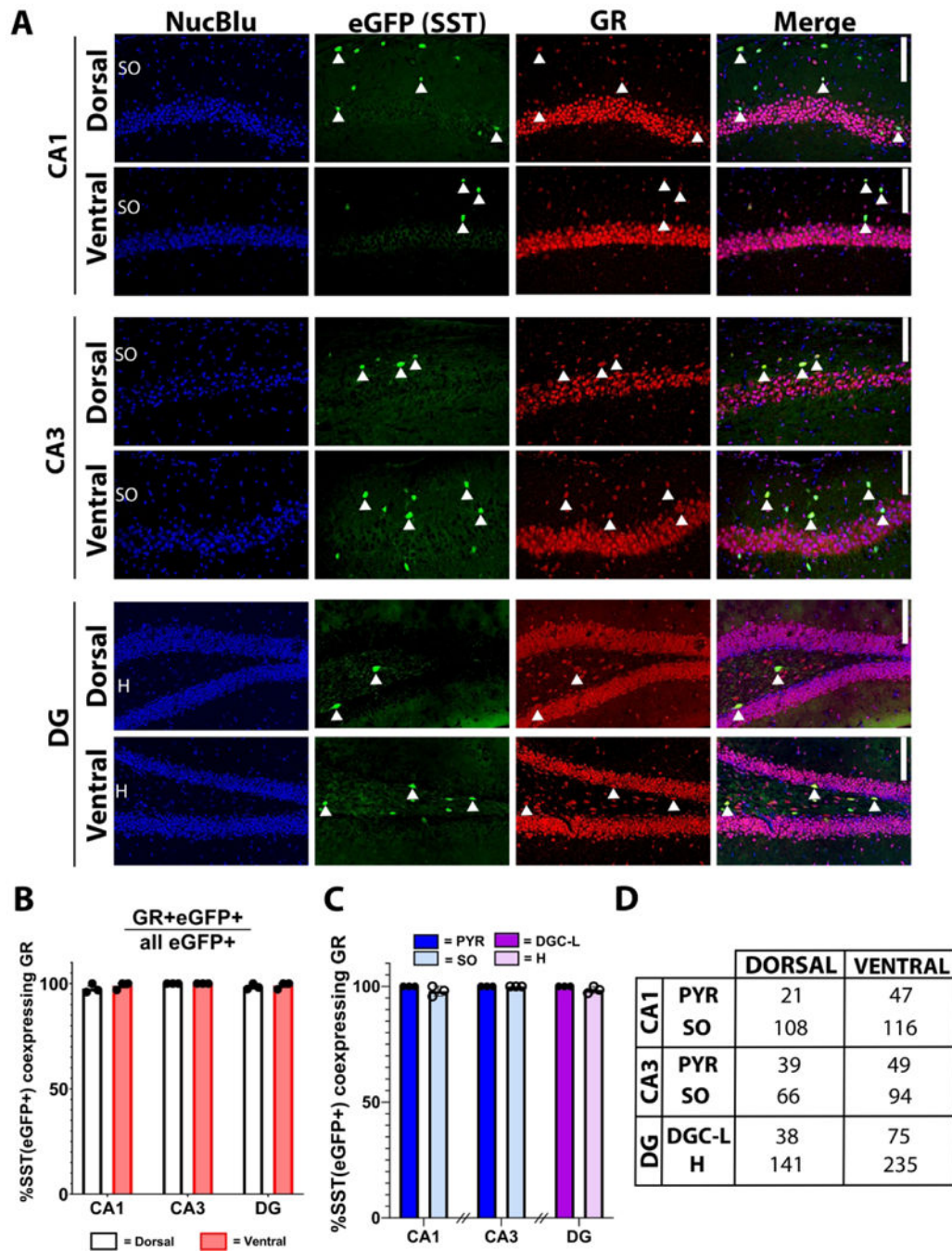
Figure 5. Hippocampal SST+ interneurons ubiquitously express GR.
A) Representative micrographs of SST+ interneuron GR expression in dorsal and ventral CAI, CA3 and dentate gyrus (DG). Solid arrowheads highlight co-expressing cells throughout the *stratum oriens* (SO), *stratum pyramidale* (PYR), dentate granule cell body layer (DGC-L) and hilus (H). Scale bar = 100 μm. **B)** Percentage of PV+ interneurons which express GR by dorsal (white) and ventral (red) hippocampal subregion. **C)** Percentage of SST+ interneurons which express GR, presented by cell layer within CAI, CA3 and DG. **D)** Cell counts (n) for each condition. Bars represent mean±SEM.
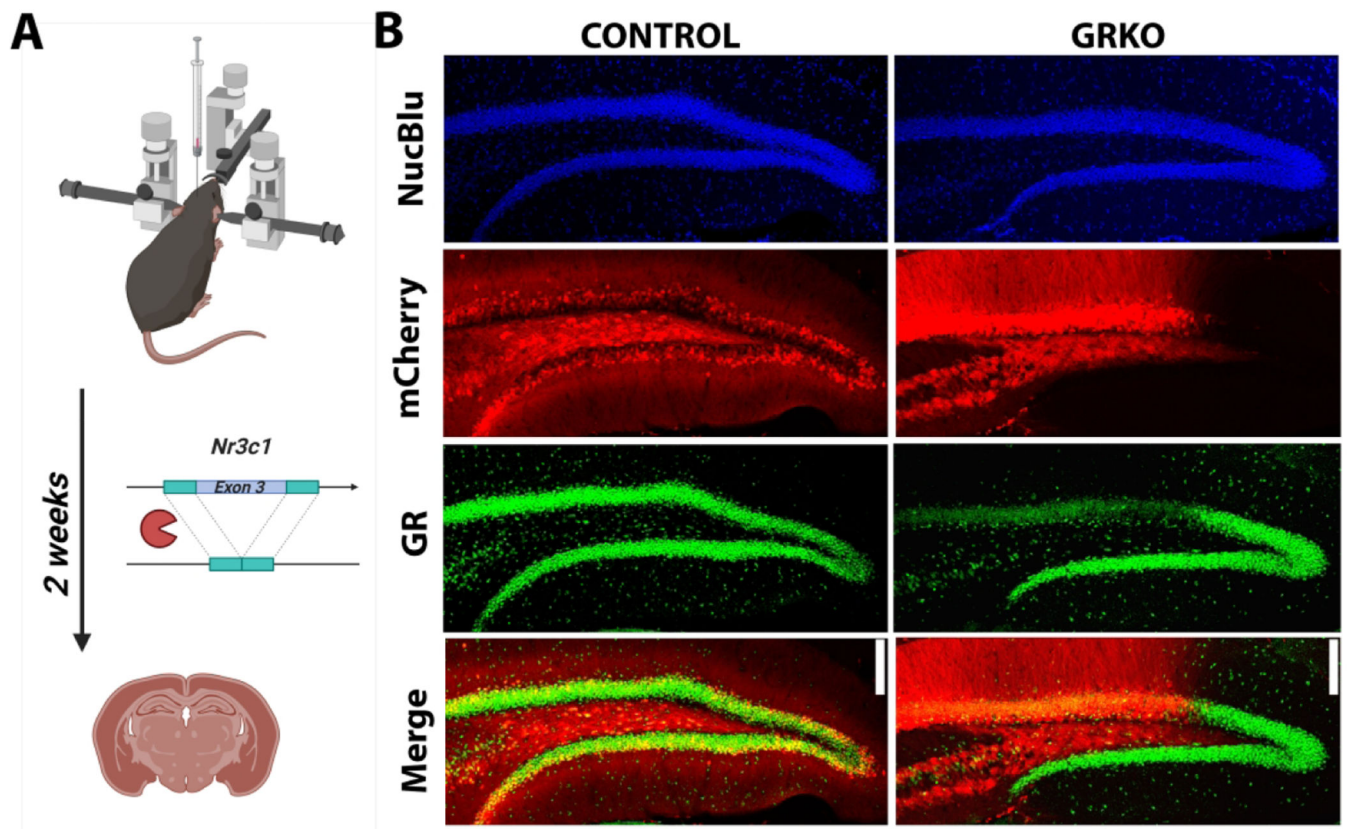
Figure 6. Biological selectivity of GR primary antibody.
A) Experimental approach and timeline for viral-mediated GR deletion representing Cre-mediated deletion of exon 3 from *Nr3c1.* **B)** Representative micrographs demonstrating preservation of GR immunoreactivity in a virus-injected control (GR$^{wt/wt}$) mouse and loss of GR from mCherry-expressing dentate granule cells in the GR knockout or GRKO (GR$^{fl/fl}$) mouse. Scale bar = 25 μm.

Table 1:

Mouse numbers, genotype, sex and the experiments the animals were used for in the present study.

GENOTYPE	N (SEX)	EXPERIMENT	GOAL
PV;eGFP	4 (2M, 2F)	1) PV + eGFP IHC 2) GR + eGFP IHC	3) Sensitivity and specificity of PV;eGFP line 4) GR expression in PV neurons
SST;eGFP	3 (2M, 1F)	3) SST + eGFP IHC 4) GR + eGFP IHC	5) Sensitivity and specificity of SST;eGFP line 6) GR expression in SST neurons
GR$^{fl/fl, wt/wt}$	2 (1M, 1M)	VIRUS + GR IHC	Positive control knockout tissue for GR antibody selectivity

Abbreviations: PV: parvalbumin, SST: somatostatin, eGFP: enhanced green fluorescent protein, GR: glucocorticoid receptor; IHC: immunohistochemistry.

Table 2.

Details on the antibodies used in the present study.

ANTIBODY	TARGET	SPECIES	CONCENTRATION	SOURCE
PRIMARIES	Parvalbumin (PV)	GUINEA PIG	1:1000 or 2 µg/mL	Synaptic Systems (Cat# 195–004, RRID:AB_2156476)
	Glucocorticoid Receptor (GR)	RABBIT	1:800 or 6.5 µ/mL	Thermo Fisher Scientific (Cat# PA5–21341, RRID:AB_11152512)
	Somatostatin (SST)	RAT	1:200 or 10 µ/mL	Millipore Sigma (Cat# MAB354, RRID:AB_2255365)
	Enhanced green fluorescent protein (eGFP)	CHICKEN	1:500 or 4 µ/mL	Abcam (Cat# AB13970, RRID:AB_300798)
Highly Cross-Adsorbed SECONDARIES	Alexa Fluor 647 antiguinea pig IgG (H+L)	GOAT	1:1000 or 2 µ/mL	Invitrogen by Thermo Fisher Scientific (Cat# A-21450, RRID:AB_2735091)
	Alexa Fluor 647 anti-rabbit IgG (H+L)	GOAT	1:1000 or 2 µ/mL	Invitrogen by Thermo Fisher Scientific (Cat# A-21244, RRID:AB_2535812)
	Alexa Fluor 568 antirat (H+L)	GOAT	1:1000 or 2 µ/mL	Invitrogen by Thermo Fisher Scientific (Cat# A-11077, RRID:AB_2534121)
	Alexa Fluor 488 antichicken (H+L)	GOAT	1:1000 or 2 µ/mL	Invitrogen by Thermo Fisher Scientific (Cat# A-32931, RRID:AB_2762843)